

# Effect of Addition of a Neutral Solvent on the Order–Order and Order–Disorder Transitions in a Polystyrene-*block*-polyisoprene-*block*-polystyrene Copolymer

Naoki Sakamoto and Takeji Hashimoto\*

Department of Polymer Chemistry, Graduate School of Engineering, Kyoto University, Sakyo-ku, Kyoto 606-01, Japan

Chang Dae Han,\* Do Kim, and Nitin Y. Vaidya

Department of Polymer Engineering, The University of Akron, Akron, Ohio 44325-0301

Received November 18, 1996; Revised Manuscript Received June 23, 1997<sup>©</sup>

**ABSTRACT:** We investigated the order–order and order–disorder transitions in a solution consisting of polystyrene-*block*-polyisoprene-*block*-polystyrene copolymer (Vector 4111 having weight-average molecular weights of  $26 \times 10^3$  and  $117 \times 10^3$  for polystyrene and polyisoprene block chains, respectively) and dioctyl phthalate (DOP), using small-angle X-ray scattering (SAXS), rheology, and transmission electron microscopy (TEM). SAXS results obtained in a heating process show (a) that, in the 85.5/14.5 weight fraction Vector 4111/DOP solution, (1) an order–order transition (OOT) takes place at 130–140 °C, (2) a lattice-disordering transition (LDT) takes place at 150–155 °C, and (3) an order–disorder transition (ODT) takes place at ca. 205 °C and (b) that, in the 73.2/26.8 Vector 4111/DOP solution, (1) an OOT takes place at 80–90 °C, (2) no LDT takes place because the structure formed after the OOT contains a considerable amount of lattice distortion, and (3) an ODT takes place at ca. 130 °C. Both SAXS and TEM results show that, in the 85.5/14.5 Vector 4111/DOP solution, hexagonally-packed cylindrical microdomains of polystyrene transform into spherical microdomains at the OOT temperature ( $T_{OOT}$ ). Comparison of SAXS results with rheological results indicates that the addition of 14.5 wt % DOP lowered both the  $T_{ODT}$  and the lattice-disordering transition temperature of bulk Vector 4111 by ca. 50 °C. By assuming that DOP strictly plays the role of diluent, we estimated the ODT temperature ( $T_{ODT}$ ) of bulk Vector 4111 to be ca. 280 °C, which supports the conclusion drawn in our previous study that the  $T_{ODT}$  of bulk Vector 4111 is much higher than 220 °C.

## Introduction

It is well established today that the order–disorder transition (ODT) temperature ( $T_{ODT}$ ) of a block copolymer depends on its composition and molecular weight.<sup>1,2</sup> Therefore, an ideal situation would be to synthesize block copolymers by first calculating the required block composition and molecular weight for a desired  $T_{ODT}$ , which is perhaps the most important parameter from the processing point of view. Note that too high a  $T_{ODT}$  for a block copolymer requires high processing temperatures, which is often not practical because cross-linking reactions (and/or thermal degradation) may take place during the processing of, for example, diene-based block copolymers (e.g., polystyrene-*block*-polybutadiene-*block*-polystyrene (SBS triblock) copolymer, polystyrene-*block*-polyisoprene-*block*-polystyrene (SIS triblock) copolymer) at temperatures higher than say 220 °C. There is an abundance of experimental evidence showing that the melt viscosity of a block copolymer in the ordered state is much higher than that in the disordered state.<sup>3–6</sup> This can be explained by an argument that the microdomains, of the order of a hundred Ångströms in size, in a block copolymer can be regarded as being equivalent to cross-linked microgels in a homopolymer.

For a given block copolymer, there are two ways of lowering its  $T_{ODT}$ : (1) by adding a low molecular weight homopolymer and (2) by adding a neutral solvent. One can easily surmise that the mechanisms associated with the two methods described above for lowering the  $T_{ODT}$  of a block copolymer are different. In the past, a number of investigators<sup>7–18</sup> reported on various phe-

nomena occurring in mixtures of block copolymer and homopolymer. When a low molecular weight homopolymer is added to a block copolymer and the mixture forms ordered domains, the homopolymer may be selectively solubilized into the corresponding microdomains of the block copolymer, giving rise to a morphological transition,<sup>7–18</sup> or may form a separate phase.<sup>13–15,18</sup> On the other hand, a neutral solvent will simply play the role of a diluent. It should be noted that effects of diluent on  $T_{ODT}$  and rheological properties of block copolymers are also important from a practical point of view, e.g., the role of tackifiers in adhesives<sup>19,20</sup> and the general use of oil-extended block copolymers.<sup>19</sup>

Very recently, using small-angle X-ray scattering (SAXS), Sakurai et al.<sup>21</sup> reported on the thermoreversibility of the morphological transition between hexagonally-packed cylinders and spherical microdomains, often referred to as the order–order transition (OOT), in a solution consisting of polystyrene-*block*-polyisoprene (SI diblock) copolymer (having weight-average molecular weights of  $13 \times 10^3$  and  $69 \times 10^3$  for polystyrene and polyisoprene block chains) and dioctyl phthalate (DOP). Note that DOP can be regarded as a neutral solvent. It should be mentioned that, earlier, an OOT in bulk block copolymer has been reported.<sup>22–28</sup>

In a recent study,<sup>29</sup> we investigated OOT and order–disorder transition (ODT) in a polystyrene-*block*-polyisoprene-*block*-polystyrene (SIS triblock) copolymer (designated as Vector 4111). We found that Vector 4111 undergoes an OOT at 182–185 °C from hexagonally-packed cylindrical microdomains of polystyrene (PS) to spherical microdomains of PS in a cubic lattice and has a  $T_{ODT}$  higher than 220 °C, the highest experimental temperature employed. Unfortunately we cannot un-

<sup>©</sup> Abstract published in *Advance ACS Abstracts*, August 15, 1997.

equivocally specify the lattice symmetry for this system. In that study we also found that Vector 4111 exhibits a unique transition, designated as the lattice-disordering transition (LDT),<sup>29,30</sup> inherent in spherical microdomain systems.<sup>31</sup> Specifically, we found that (1) at temperatures above the order–order transition temperature ( $T_{OOT}$ ) but below the lattice-disordering transition temperature ( $T_{LDT}$ ) the spheres were spatially arranged in a cubic lattice with a long range spatial order and (2) at temperatures above the  $T_{LDT}$  but below the  $T_{ODT}$ , however, the spheres lost the long range order and had only a liquid-like short range order. Thus LDT is an order–disorder transition of spherical microdomains. Note that the spherical microdomain with a sharp interface still exists even above the LDT (but below the ODT), as will be clarified later, and that it will eventually disappear above a critical temperature, which we designate as  $T_{ODT}$ .

It should be mentioned that the existence of a LDT in a block copolymer having spherical microdomains was first reported by Hashimoto et al.<sup>30</sup> more than a decade ago. In order to facilitate our discussion later in this paper, at this juncture we wish to emphasize the distinction between LDT and ODT, although its necessity is well borne out in our previous paper.<sup>29</sup> We believe that this distinction is necessary because the spherical microdomains clearly exist at temperatures between  $T_{LDT}$  and  $T_{ODT}$  and they have an interface nearly as sharp as that below  $T_{LDT}$ , as elucidated in our previous paper.<sup>29</sup> The latter evidence is based on the observation that the asymptotic behavior of the scattering intensity distribution with respect to the magnitude of the scattering vector  $q$  in a high- $q$  region is essentially unaltered while crossing  $T_{LDT}$ . In order to help observation of asymptotic behavior, we added straight lines in the figure showing the asymptotic behavior of  $q^{-4}$  and  $q^{-2}$ . Thus we should distinguish the spherical microdomains existing at temperatures between  $T_{LDT}$  and  $T_{ODT}$  from the concentration fluctuations which may take place at temperatures above  $T_{ODT}$ ,<sup>1,32</sup> i.e., at temperatures above  $T_{ODT}$  the spheres with the sharp interface disappear and they transform into thermal concentration fluctuations. The sharp interface in the spherical microdomains of a block copolymer is not expected when concentration fluctuations take place in the disordered state (at  $T > T_{ODT}$ ). At temperatures below  $T_{ODT}$ , the spheres with the sharp interface may be packed in a body-centered cubic lattice, if the random thermal force is weak compared to the force forming the lattice, as in the case of the Landau-type mean-field theory.<sup>1</sup> In the regime where the Landau-type mean-field theory holds, the LDT and the ODT are identical. However if the random thermal force outweighs the force forming the lattice, the lattice is destroyed but the spheres can yet exist with a short range liquid-like order; thus, the LDT and the ODT are split.

In the present study, we investigated the high-temperature behavior of an SIS triblock copolymer (Vector 4111) by extending the effective temperature range that can be covered experimentally without significant thermal degradation effects. In our previous study<sup>29</sup> which also used Vector 4111, the highest experimental temperature employed was 220 °C because there is experimental evidence<sup>6</sup> suggesting that cross-linking reactions may take place in SI diblock and SIS triblock copolymers at temperatures above 220 °C. In this regard, it should be pointed out that any experimental data for diene-based block copolymers, which were taken at temperatures above ca. 220 °C, can

be regarded as being influenced by cross-linking reactions. In the present study, the extension of the high-temperature range was achieved by lowering the  $T_{ODT}$  of Vector 4111 with the addition of a neutral solvent, DOP;<sup>33</sup> specifically, we were interested in estimating the  $T_{ODT}$  of bulk Vector 4111 from the measurement of  $T_{ODT}$  of Vector 4111 diluted with DOP. In so doing, we investigated the effect of addition of a neutral solvent on the OOT, the LDT, and the ODT in Vector 4111, using SAXS, rheology, and transmission electron microscopy (TEM). In this paper we report the highlights of our findings.

## Experimental Section

**Materials.** We employed an SIS triblock copolymer (Vector 4111, Dexco Polymers Company), which has (i) the weight-average molecular weight  $1.4 \times 10^5$ , as determined by light scattering, (ii) a 0.183 weight fraction of polystyrene blocks, as determined by nuclear magnetic resonance spectroscopy, and (iii) the polydispersity index ( $M_w/M_n$ ) 1.11, as determined by gel permeation chromatography. Solutions consisting of 85.5 wt % Vector 4111 and 14.5 wt % DOP (designated as 85.5/14.5 Vector 4111/DOP) and consisting of 73.2 wt % Vector 4111 and 26.8 wt % DOP (designated as 73.2/26.8 Vector 4111/DOP) were prepared using the following procedures. (1) Predetermined amounts of Vector 4111 and DOP were mixed into toluene in the presence of an antioxidant (Irganox 1010, Ciba-Geigy Group) to give a 10 wt % homogeneous solution. The amount of antioxidant added to the specimen was 0.1 wt %. (2) The solvent was evaporated slowly in a fume hood for 1 week and then in a vacuum oven at room temperature for 4 days. (3) The sample was further dried in the vacuum oven at 40 °C for 3 days. (4) The temperature was raised gradually at a rate of 10 °C/h up to 100 °C. (5) The drying of the sample was continued until there was no weight change. The final weight and predetermined amount of Vector 4111 determined the polymer concentration.

**SAXS Experiment.** SAXS experiments were conducted under a nitrogen atmosphere for the heating and cooling cycles, using an apparatus described in detail elsewhere.<sup>35</sup> The SAXS apparatus consists of an 18-kW rotating-anode X-ray generator (MAC Science, Japan), a graphite crystal for incident-beam monochromatization, a 1.5-m camera, and a one-dimensional position-sensitive proportional counter. The Cu K $\alpha$  line ( $\lambda = 0.154$  nm) was used. The SAXS profiles were measured *in situ* as a function of temperature. As-cast films were used for the experiments in the heating cycle for both 85.5/14.5 and 73.2/26.8 Vector 4111/DOP specimens. At each temperature, the specimens were held for 15 min before measurement began and then the measurement lasted for 45 min. In the cooling cycle for both 85.5/14.5 and 73.2/26.8 Vector 4111/DOP mixtures, the specimen was first annealed for 1 h at 220 °C and then used for SAXS measurement. At each temperature, the specimen was held for 20 min before measurement began and then the measurement lasted for 30 min. The SAXS profiles were corrected for absorption, air scattering, and background scattering, arising from thermal diffuse scattering, and for slit-height and slit-width smearing.<sup>36</sup> The absolute SAXS intensity was obtained using the nickel-foil method.<sup>37</sup>

**Rheological Measurement.** Rheological measurements were taken of the 85.5/14.5 Vector 4111/DOP solution using a Rheometrics Mechanical Spectrometer (Model RMS 800) in the oscillatory mode with parallel plate fixtures (25 mm diameter). Two different types of experiment were conducted. (1) Dynamic temperature sweep experiments were conducted at an angular frequency ( $\omega$ ) of 0.01 rad/s with temperatures increasing from 100 to 210 °C at a rate of 0.4 °C/min. (2) Dynamic frequency sweep experiments were conducted; i.e., dynamic storage and loss moduli ( $G'$  and  $G''$ ) were measured as functions of angular frequency ( $\omega$ ) ranging from 0.01 to 100 rad/s by heating a specimen from 100 to 210 °C. The temperature increment in the frequency sweep experiment varied from 3 to 10 °C, and the specimen was kept at a constant temperature for 30–40 min before rheological measurements actually began. The temperature control was

**Table 1. Thermal Histories of the 85.5/14.5 Vector 4111/DOP Specimens Used for TEM Experiments**

sample code	thermal history
sample A	annealed at 120 °C for 3 days followed by a rapid quenching in ice water
sample B	annealed at 145 °C for 10 h followed by a rapid quenching in ice water
sample C	annealed at 155 °C for 1 h followed by a rapid quenching in ice water
sample D	annealed at 200 °C for 1 h followed by a rapid quenching in ice water

accurate to within  $\pm 1$  °C, and a fixed strain of 0.04 was used at a given temperature, to ensure that measurements were taken well within the linear viscoelastic range of the materials investigated. All of the rheological measurements were conducted under a nitrogen atmosphere in order to avoid oxidative degradation of the samples. The sample was annealed at 110 °C for 10 h. Before rheological measurement, each sample was annealed further at 120 °C for 1 day and quenched rapidly in ice water, and the sample was then kept in the refrigerator. The annealing at 120 °C tends to form well-ordered hexagonally-packed cylindrical microdomains of polystyrene (PS), as will be clarified below. In the present study rheological measurements were not taken at temperatures above 210 °C, since an earlier study<sup>6</sup> indicated that appreciable cross-linking reactions may take place in SI diblock or SIS triblock copolymers at temperatures higher than 220 °C even in the presence of an antioxidant.

**TEM.** TEM was conducted to determine the microdomain structure of the 85.5/14.5 Vector 4111/DOP solution. For this purpose, we annealed as-cast specimens at predetermined temperatures guided by SAXS and rheological measurements, using a high-performance vacuum oven (Yamato Scientific Co., Model DP-22), which controlled the temperature and also provided temperature uniformity inside the vacuum oven within  $\pm 1.5$  °C at 240 °C. The annealed samples were rapidly quenched in ice water. The thermal histories of the specimens used for the TEM study are summarized in Table 1. The ultrathin sectioning of the quenched specimens was performed by cryoultramicrotomy at  $-100$  °C, using a Richert Ultracut S low-temperature sectioning system. A transmission electron microscope (JEM 1200EX II, JEOL) operated at 100 kV was used for taking morphological images of the specimens stained with osmium tetroxide vapor.

## Results and Discussion

**SAXS Study.** Figure 1 gives SAXS profiles for the 85.5/14.5 Vector 4111/DOP solution at various temperatures in the heating cycle, where  $q$  is the magnitude of the scattering vector defined by  $q = (4\pi/\lambda) \sin(\theta/2)$  with  $\lambda$  and  $\theta$  being the wavelength of the X-rays and the scattering angle, respectively. In Figure 1 we make the following observations. (1) The ratio of peak position changes from  $1:\sqrt{3}:\sqrt{4}$  to  $1:\sqrt{2}:\sqrt{3}$  as the temperature increases from 130 to 140 °C, indicating that an OOT from hexagonally-packed cylindrical microdomains of PS to spherical microdomains packed in a cubic lattice takes place in this temperature interval. It should be mentioned that the  $T_{OOT}$  determined from the SAXS experiment in the cooling cycle, although not shown here, was between 125 and 130 °C. (2) The widths of the first- and higher-order peaks increase with increasing temperature, but the increase of the peak width with increasing temperature becomes discontinuous, as will be elaborated on below, at  $T_{OOT}$  and, also, at  $T_{LDT}$ , which lies between 150 and 155 °C. Upon increasing the temperature across  $T_{LDT}$ , the spheres of PS in a cubic lattice are transformed into the spheres of PS with short-range liquid-like order (designated hereafter as 'disordered spheres'). Notice in Figure 1 that the SAXS profile at 155 °C still shows higher-order peaks or shoulders, implying that the system still has a disor-

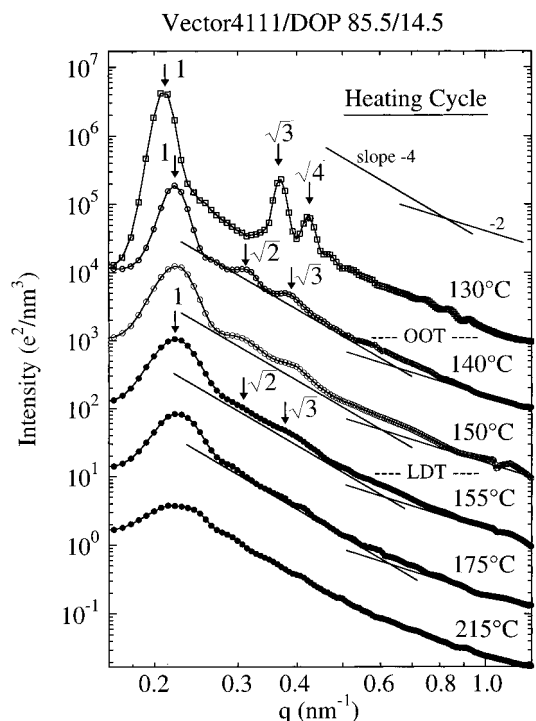


**Figure 1.** Temperature dependence of SAXS profiles for the 85.5/14.5 Vector 4111/DOP solution during heating at various temperatures indicated on the plot. The intensities of the profile shown at the top of this figure are actually measured values, and in order to avoid overlaps, the intensities of other profiles were shifted down by one decade relative to the intensities immediately above. The arrows on the profiles show the expected positions for the higher-order scattering maxima. The straight line having a slope of  $-4$  is drawn to each SAXS profile to show the asymptotic behavior of  $I(q) \sim q^{-4}$ , while the straight line of slope  $-2$  is drawn to each SAXS profile as a guide to the eye for the crossover behavior from  $q^{-4}$  to  $q^{-2}$ .

dered cubic lattice at 155 °C, i.e., at a temperature higher than but near  $T_{LDT}$ . The lattice distortion at this temperature is much larger than that below  $T_{LDT}$ . As the temperature is increased further, the lattice distortion increases further, and the system has spheres with short-range liquid-like order. (3) At  $T \geq 215$  °C there is no higher order peak, indicating that the 85.5/14.5 Vector 4111/DOP solution is in a completely disordered state at which PS and PI blocks are mixed on the molecular level and hence no spherical microdomains exist.

In some spherical microdomain systems,<sup>38</sup> especially those for high molecular weights, the scattering maxima from the sphere form factor appear. Unfortunately, however, the system under consideration here does not show the maxima, presumably due to smaller molecular weight and hence smaller segregation power compared to that for the system showing the maxima. This makes an assessment on whether or not the spheres exist difficult. Since the average radius of spheres cannot be estimated from the sphere form factor, we cannot estimate the volume fraction of spheres and hence the symmetry of the cubic lattice of our system.

Figure 2 gives plots of (a) the reciprocal of the first-order peak intensity ( $1/I_m$ ) versus the reciprocal of the absolute temperature ( $1/T$ ), the square of the half-width at half maximum ( $\sigma_q^2$ ) of the SAXS profile versus  $1/T$ , and (b) the Bragg spacing ( $D = 2\pi/q_m$ ,  $q_m$  being the value of  $q$  at the first-order scattering maximum) versus  $1/T$  for the 85.5/14.5 Vector 4111/DOP solution, at temperatures ranging from 110 to 220 °C during the heating cycle. In Figure 2 we observe that all three quantities,

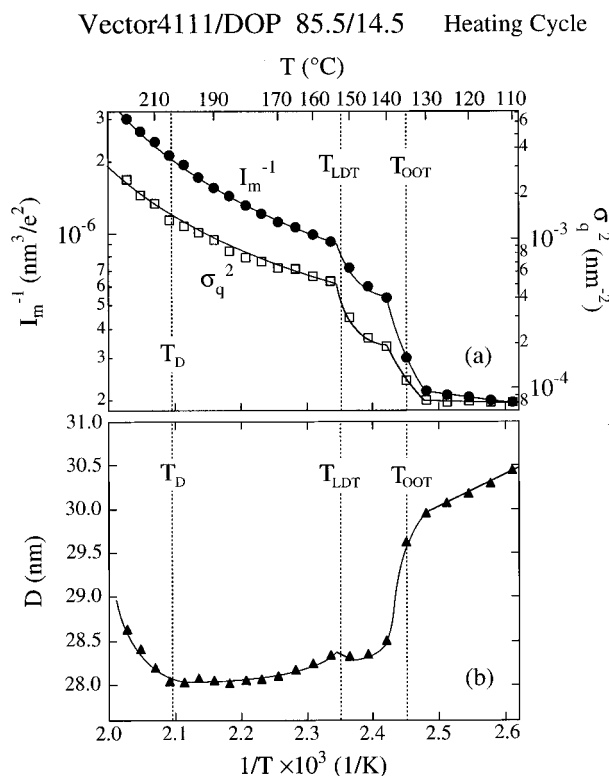


**Figure 2.** Plots of (a)  $1/I_m$  versus  $1/T$  (●),  $\sigma_q^2$  versus  $1/T$  (□), and (b)  $D$  versus  $1/T$  (▲) which were prepared from SAXS experiments conducted during heating, for the 85.5/14.5 Vector 4111/DOP solution. The lines are drawn through the data points as a guide.  $T_{OOT}$ ,  $T_{LDT}$ , and  $T_D$  designate, respectively, order–order transition temperature, lattice-disordering transition temperature, and a temperature above which  $D$  or  $I(q)$  at  $q < q_m$  starts to increase. We speculate that  $T_D$  is equivalent to  $T_{ODT}$ .

$1/I_m$ ,  $\sigma_q^2$ , and  $D$ , have a more or less discontinuous change at 130–140 °C, which describes  $T_{OOT}$ , and another similarly shaped discontinuity at 150–155 °C, which describes  $T_{LDT}$ . More precisely stated, we observe that  $1/I_m$  and  $\sigma_q^2$  start to increase and  $D$  starts to decrease rapidly with increasing temperature above 130 °C and that these rapid changes continue to 140 °C. This observation indicates that the OOT starts at 130 °C and is completed at ca. 140 °C. The data point at 135 °C may indicate a co-existence of hexagonally-packed cylindrical microdomains of PS and spherical microdomains of PS. With a further increase of temperature above 140 °C,  $1/I_m$  and  $\sigma_q^2$  start again to increase rapidly at about 150 °C and continue to ca. 155 °C, suggesting the onset and completion of the LDT at ca. 150 and 155 °C, respectively. Although in Figure 2 the discontinuity in  $D$  at  $T_{LDT}$  is less obvious compared to that at  $T_{OOT}$ , we expect that the discontinuity exists as reported in the previous paper.<sup>29</sup> In other words the cusp at ca. 155 °C in  $D$  versus  $1/T$  is expected to become clear, if the temperature increment in the experiment is made smaller as in the case of our previous work.<sup>29</sup>

We can conclude from the above observations that the addition of a neutral solvent, DOP, in the amount of 14.5 wt % certainly lowered both the  $T_{OOT}$  (179–185 °C) and the  $T_{LDT}$  (210–212 °C) of bulk Vector 4111.<sup>29</sup> In Figure 2, however, we observe a very unusual trend that  $D$  increases as the temperature is increased above 205 °C, whereas  $1/I_m$  and  $\sigma_q^2$  do not show such an obvious anomaly in the same temperature range.

SAXS profiles at temperatures above 150 °C are given in Figure 3, where the peak position hardly changes with temperature up to about 205 °C but shifts to a

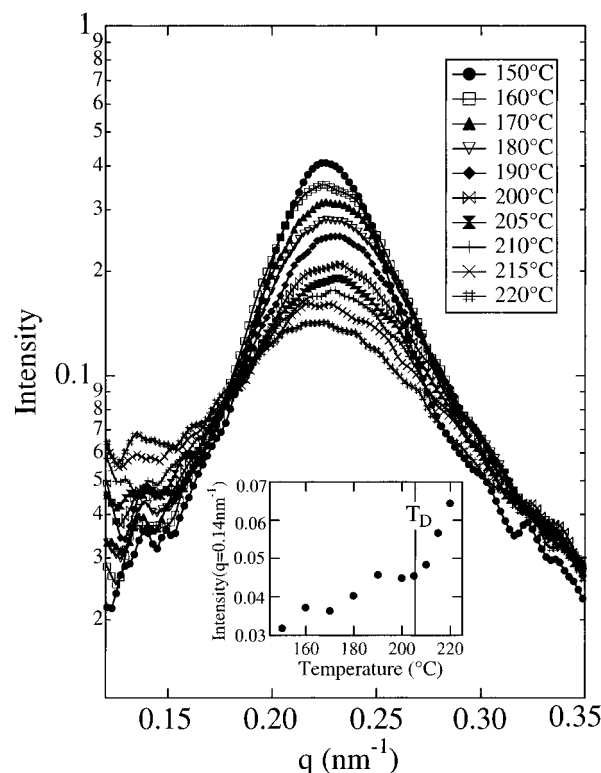


**Figure 3.** SAXS profiles near the first-order peak for the 85.5/14.5 Vector 4111/DOP solution during heating at various temperatures above 150 °C. The inset shows the temperature dependence of  $I(q)$  at  $q = 0.14 \text{ nm}^{-1}$ .

smaller  $q$  value with a further increase of temperature above 205 °C. At present we can only speculate that this unusual behavior at  $T > 205$  °C may be associated with the osmotic compressibility of the 85.5/14.5 Vector 4111/DOP solution investigated. Note that the osmotic compressibility in a block copolymer solution consists of two components: (1) the osmotic compressibility between component block chains (component I) and (2) the osmotic compressibility between block chains and solvent molecules (DOP in the present situation) (component II). We speculate that, in the high-temperature range above 205 °C, the contribution of component II to the scattering becomes increasingly important compared to the contribution of component I: concentration fluctuations between Vector 4111 and DOP increase while concentration fluctuations between polystyrene blocks and polyisoprene blocks decrease. The scattering arising from component II gives rise to a scattering maximum at  $q = 0$ , while the scattering arising from component I gives rise to a scattering maximum at  $q = q_m$ . Therefore the increasing contribution of component II to the net scattering may shift the scattering maximum due to component I to a smaller  $q$  value, giving rise to the apparent decrease of  $q_m$  and hence increase of  $D$ , as observed in Figure 2b. The trend that the intensity at  $q$  (e.g.,  $1.4 \times 10^{-1} \text{ nm}^{-1}$ ) smaller than  $q_m$  increases, and the intensity at  $q = q_m$  decreases with increasing temperature is clearly shown in Figure 3. This tendency will become greater as the temperature increases, and the contribution of component II will grow while the Vector 4111/DOP solution undergoes an ODT. If at  $T > 205$  °C the system goes into the disordered state, this may further increase the contribution of component II.

Thus we are led to tentatively conclude that the  $T_{ODT}$  of the 85.5/14.5 Vector 4111/DOP solution is ca. 205 °C. We assume that the unusual behavior at 205 °C is due to a ODT. It is important to note that this ODT, where

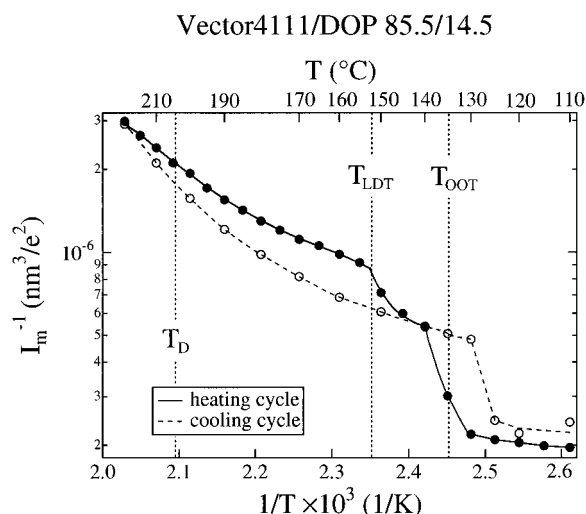


**Figure 4.** Plots of  $1/I_m$  versus  $1/T$  which were prepared from SAXS experiments conducted during heating (●) and cooling (○), respectively, for the 85.5/14.5 Vector 4111/DOP solution. The solid and broken lines are drawn through the data points as a guide.

the spherical microdomains are dissolved into a homogeneous molecular mixture of the constituent block chains, occurs continuously and does not invoke the discontinuous changes in  $I_m^{-1}$  and  $\sigma_q^2$ , as observed in the ODT in lamellar systems.<sup>39</sup> The same trend will be seen for the 73.1/26.8 Vector 4111/DOP system.

Using the values of  $T_{OOT}$  and  $T_{LDT}$  thus obtained for 85.5/14.5 Vector 4111/DOP solution, we calculated reduced values of  $T_{OOT}$  defined by  $T_{OOT,r} = T_{OOT}/\phi_p$  and reduced values of  $T_{LDT}$  defined by  $T_{LDT,r} = T_{LDT}/\phi_p$ , where  $\phi_p$  is the volume fraction of the block copolymer in the solution. Thus,  $T_{OOT,r}$  corresponds to the  $T_{OOT,bulk}$  of Vector 4111, and  $T_{LDT,r}$  corresponds to the  $T_{LDT,bulk}$  of Vector 4111. In so doing, we implicitly assumed that (1)  $\chi_{eff} = \chi\phi_p$ ,<sup>40,41</sup> where  $\chi_{eff}$  is the effective interaction parameter between styrene and isoprene segments in the presence of DOP and  $\chi$  is the interaction parameter between styrene and isoprene segments for bulk Vector 4111; (2)  $\chi \sim 1/T$ ; and (3)  $\chi_{eff} \sim \phi_p/T$ .<sup>40,41</sup> We obtained  $T_{OOT,r} = 204^\circ\text{C}$  and  $T_{LDT,r} = 227^\circ\text{C}$ . These values are about  $20^\circ\text{C}$  higher than those ( $T_{OOT,bulk} = 182^\circ\text{C}$  and  $T_{LDT,bulk} = 212^\circ\text{C}$ ) obtained for bulk Vector 4111 in our previous study.<sup>29</sup> The agreement seems reasonable in view of the accuracy of the approximations employed. Moreover, if we define  $T_D$  as the temperature at which  $D$  starts to increase (see the vertical broken line drawn at  $1/T \approx 2.1 \times 10^{-3} \text{ K}^{-1}$  in Figure 2b), then reduced values of  $T_D$  can be estimated from  $T_{D,r} = T_D/\phi_p$ . Since  $T_D$  is  $205^\circ\text{C}$  for the 85.5/14.5 Vector 4111/DOP solution, we have  $T_{D,r} = 287^\circ\text{C}$ . If we assume that the  $T_D$  of the 85.5/14.5 Vector 4111/DOP solution corresponds to its  $T_{ODT}$ ,  $T_{D,r} = 287^\circ\text{C}$  corresponds to the  $T_{ODT}$  of bulk Vector 4111. This estimate is consistent with the conclusion drawn in our previous study<sup>29</sup> that the  $T_{ODT}$  of Vector 4111 is higher than  $220^\circ\text{C}$ , the highest experimental temperature employed. For more rigorous analysis<sup>42</sup> one must be concerned with the accuracy of the dilution approximation made above.

Figure 4 gives plots of  $1/I_m$  versus  $1/T$  during the heating (●) and cooling (○) cycles. Figure 5 gives plots of  $\sigma_q^2$  versus  $1/T$  during the heating (■) and cooling (□) cycles, and Figure 6 gives plots of  $D$  versus  $1/T$  during the heating (▲) and cooling (△) cycles, at temperatures ranging from 110 to  $220^\circ\text{C}$ . The scattering profiles obtained during the cooling cycle, similar to Figure 1, are not shown here. The change of the profile with

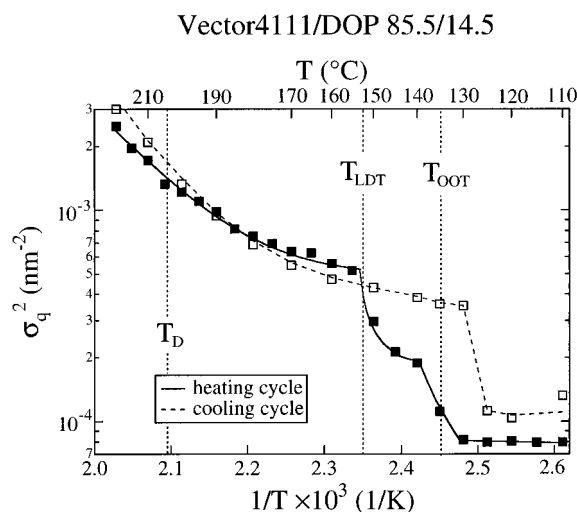


**Figure 5.** Plots of  $\sigma_q^2$  versus  $1/T$  which were prepared from SAXS experiments conducted during heating (■) and cooling (□), respectively, for the 85.5/14.5 Vector 4111/DOP solution. The solid and broken lines are drawn through the data points as a guide.

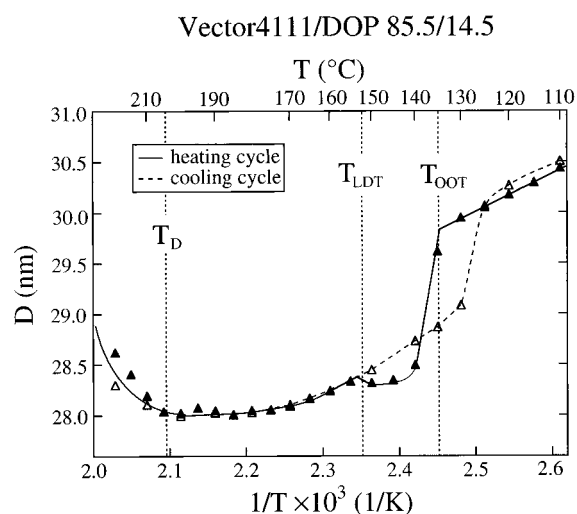


**Figure 6.** Plots of  $D$  versus  $1/T$  which were prepared from SAXS experiments conducted during heating (▲) and cooling (△), respectively, for the 85.5/14.5 Vector 4111/DOP solution. The solid and broken lines are drawn through the data points as a guide.

temperature is very similar to that shown in Figure 4 of ref 29. The following observations are worth noting in Figures 4–6: (1) the values of  $T_{OOT}$  obtained in the heating and cooling cycles agree to within  $10^\circ\text{C}$ ; (2) at temperatures below  $T_{LDT}$ , the temperature dependencies of  $\sigma_q^2$  and  $D$  during the heating cycle are different from those during the cooling cycle; (3) at temperatures above  $T_{LDT}$  ( $\approx T_D$ ), the temperature dependencies of  $\sigma_q^2$  and  $D$  are almost the same during both the heating and cooling cycles; (4)  $1/I_m$ ,  $\sigma_q^2$ , and  $D$  show no change at  $T_{LDT}$  during the cooling cycle. The above observations lead us to conclude that (1) the formation of long range order by cooling requires a longer time than the disruption of long range order induced by increasing temperature and (2) the microdomain structures in the heating and cooling cycles are the same at  $T > T_{LDT}$  and in the cooling cycle no transition occurs at  $T_{LDT}$  in the time scale of our observation and thus the microdomain structure changes directly from disordered spheres to hexagonally-packed cylinders of PS. These conclusions are very similar to those made earlier for bulk Vector 4111.<sup>29</sup>

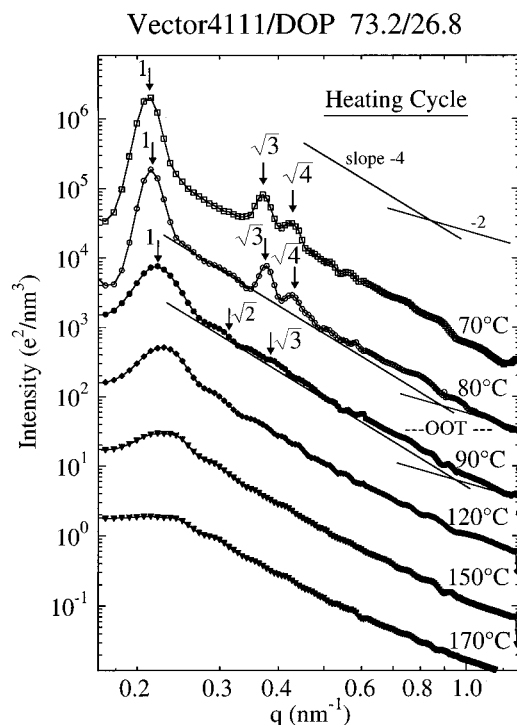


**Figure 7.** Temperature dependence of SAXS profiles for the 73.2/26.8 Vector 4111/DOP solution during heating at various temperatures indicated on the plot. The intensities of the profiles shown at top of this figure are actually measured values, and in order to avoid overlaps, the intensities of other profiles were shifted down by one decade relative to the intensities immediately above. The arrows on the profiles show the expected positions for the higher order scattering maxima. The two straight lines drawn to each SAXS profile have the same physical meanings as those in Figure 1.

Figure 7 gives SAXS profiles for the 73.2/26.8 Vector 4111/DOP solution at various temperatures in the heating cycle, and Figure 8 gives plots of (a)  $1/I_m$  versus  $1/T$  (●),  $\sigma_q^2$  versus  $1/T$  (□), and (b)  $D$  versus  $1/T$  (▲) for the 73.2/26.8 Vector 4111/DOP solution, at temperatures ranging from 50 to 160 °C in the heating cycle. In Figure 7 we observe that the sharp peaks located at  $1:\sqrt{3}:\sqrt{4}$  relative to the first-order peak change to the broad peak and shoulders located at  $1:\sqrt{2}:\sqrt{3}$  as the temperature is increased from 80 to 90 °C. This result along with the result for the 85.5/14.5 Vector 4111/DOP solution may indicate that an OOT from hexagonally-packed cylindrical microdomains of PS to spherical microdomains of PS in a distorted cubic lattice with a large paracrystalline distortion of the second kind<sup>43</sup> (i.e., *disordered spheres*) takes place in this temperature interval. The following observations are worth noting in Figures 7 and 8. (1) A discontinuous change in  $I_m$ ,  $\sigma_q^2$ , and  $D$  occurs at temperatures between 80 and 90 °C, suggesting that the  $T_{OOT}$  of the 73.2/26.8 Vector 4111/DOP solution lies between 80 and 90 °C. This value is about 50 °C lower than the  $T_{OOT}$  of the 85.5/14.5 Vector 4111/DOP solution, indicating that an increase in the amount of added DOP further decreases the  $T_{OOT}$  of bulk Vector 4111. (2) No distinct peaks at  $\sqrt{2}$  and  $\sqrt{3}$  are discernible at temperatures above 90 °C, suggesting that hexagonally-packed cylindrical microdomains of PS transform directly to disordered spherical microdomains or spheres in a considerably distorted cubic lattice at  $T_{OOT}$ ; i.e., no LDT is discernible. Very broad peaks at  $\sqrt{2}$  and  $\sqrt{3}$  still exist at temperatures close to but above  $T_{OOT}$  (e.g. 90 °C), but they are as broad as those at 155 °C in Figure 1. Having the disordered spheres at temperatures above  $T_{OOT}$  is also

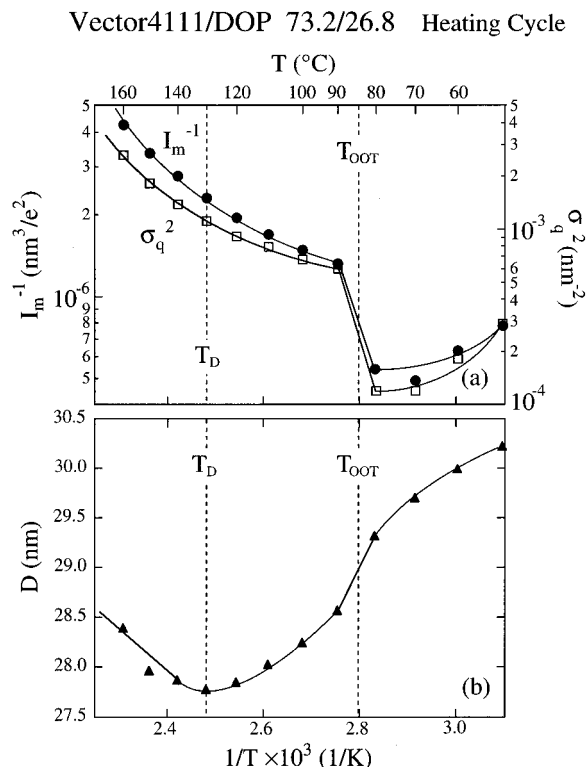
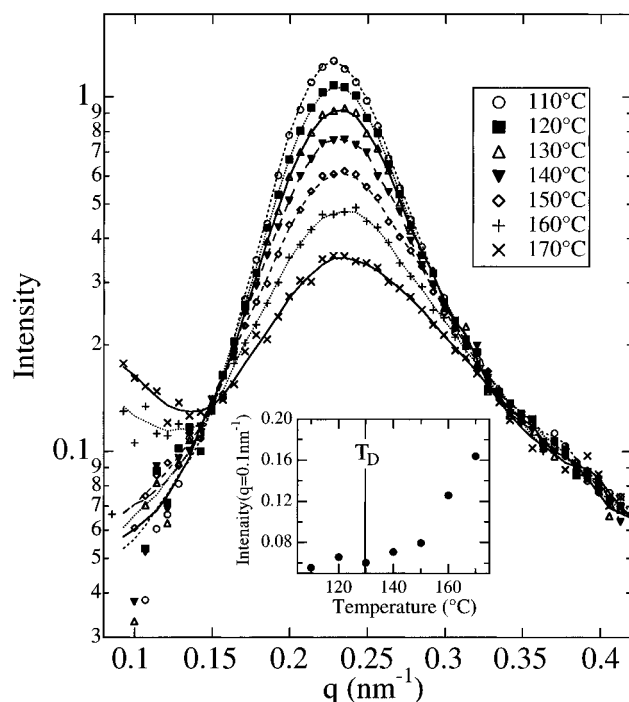


**Figure 8.** Plots of (a)  $1/I_m$  versus  $1/T$  (●),  $\sigma_q^2$  versus  $1/T$  (□), and (b)  $D$  versus  $1/T$  (▲) which were prepared from SAXS experiments conducted during heating for the 73.2/26.8 Vector 4111/DOP solution. The solid lines are drawn through the data points as a guide.  $T_{OOT}$  and  $T_D$  have the same meanings as those in Figure 2.

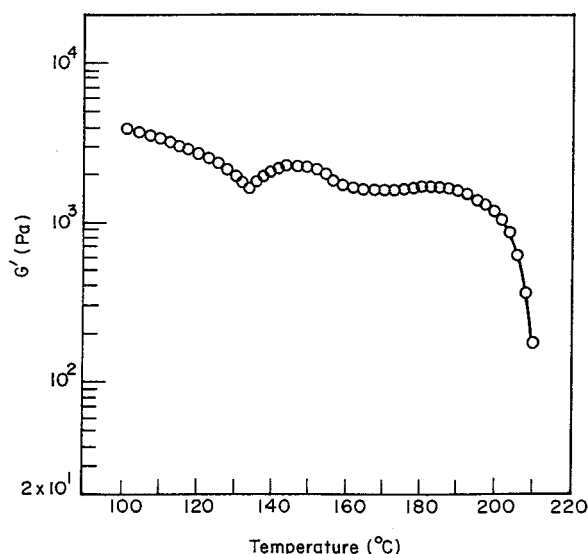
clear by comparing  $\sigma_q^2$  at 90 °C ( $6 \times 10^{-4} \text{ nm}^{-2}$ ) in Figure 8a with  $\sigma_q^2$  at 155 °C ( $5 \times 10^{-4} \text{ nm}^{-2}$ ) in Figure 2a. (3)  $D$  increases as the temperature is increased above 130 °C, behavior very similar to that observed in Figure 2b for the 85.5/14.5 Vector 4111/DOP solution. Using  $T_D = 130$  °C for the 73.2/26.8 Vector 4111/DOP solution, we estimate the value of  $T_{D,bulk}$  to be 277 °C, which corresponds to the  $T_{ODT}$  of bulk Vector 4111. This value is very close to that (287 °C) estimated from the  $T_D = 205$  °C of the 85.5/14.5 Vector 4111/DOP solution.

Figure 9 shows SAXS profiles near the first-order peak for 73.2/26.8 vector 4111/DOP, at various temperatures above 110 °C. We can observe the same trend as that seen in Figure 3 for 85.5/14.5 Vector 4111/DOP: with increasing temperature, the concentration fluctuations between the two block chains decrease, giving rise to decreasing  $I_m$ , but the concentration fluctuations between the block copolymers and solvent increase, giving rise to increasing  $I(q)$  at  $q \approx 0$ . The increase of the intensity at  $q \approx 0$  and the decrease of the intensity at  $q = q_m$  with temperature may cause a shift of the first-order peak toward low  $q$  and hence an increase of  $D$  at temperatures higher than 130 °C. This temperature of  $T_D = 130$  °C is consistent with the temperature at which  $I(q)$  at  $q = 0.1 \text{ nm}^{-1}$  ( $q < q_m$ ) starts to increase (see the inset in Figure 9). As discussed earlier, we tentatively assume that  $T_D$  is close to  $T_{ODT}$ . The  $T_{ODT}$  thus assessed is close to the  $T_{ODT}$  determined by rheological methods, as will be described below.

**Rheology Study.** Figure 10 describes the temperature dependence of the dynamic storage modulus ( $G'$ ), which was obtained by dynamic temperature sweep experiments under isochronal conditions (at  $\omega = 0.01 \text{ rad/s}$ ), during heating from 100 to 210 °C at a rate of 0.4 °C/min, for the 85.5/14.5 Vector 4111/DOP solution.



**Figure 9.** SAXS profiles near the first-order peak for the 73.2/26.8 Vector 4111/DOP solution during heating at various temperatures above 110 °C. The inset shows the temperature dependence of  $I(q)$  at  $q = 0.1 \text{ nm}^{-1}$ .



**Figure 10.** Temperature dependence of  $G'$ , under isochronal conditions at  $\omega = 0.01 \text{ rad/s}$  during heating for the 85.5/14.5 Vector 4111/DOP solution which was annealed at 140 °C for 2 days.

Notice in Figure 10 that a minimum in  $G'$  occurs at ca. 135 °C. In accordance with the rheological criterion suggested by Hamley et al.,<sup>25</sup> the temperature at which a minimum in  $G'$  occurs during a dynamic temperature sweep experiment under isochronal conditions may signify an onset of an OOT. If we apply such a rheological criterion to Figure 10, we determine the  $T_{\text{OOT}}$  of the 85.5/14.5 Vector 4111/DOP solution to be ca. 135 °C, which is very close to the value determined by SAXS experiments. Notice that in Figure 10 we observe a very mild minimum in  $G'$ , which spans over a very wide range of temperatures from 160 to 180 °C. It is not clear whether the temperature at which this mild minimum of  $G'$  occurs is related to an onset of the LDT of the 85.5/14.5 Vector 4111/DOP solution, which, according to the SAXS results presented above (see Figure 2), takes place

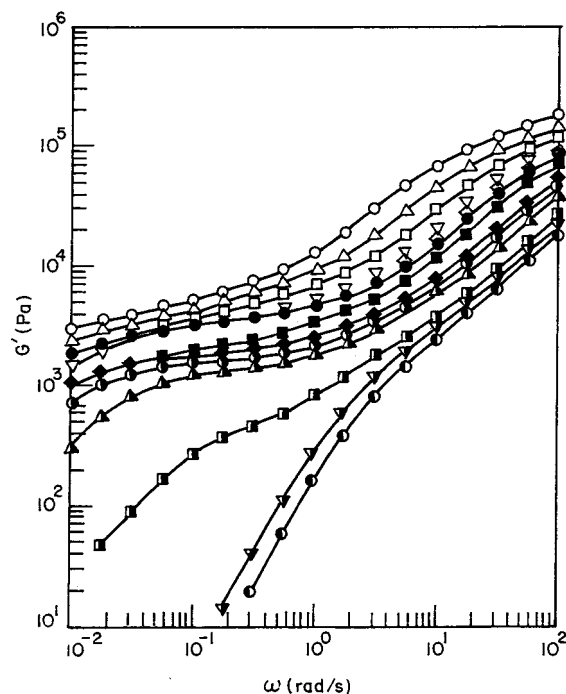


**Figure 11.** Plots of  $\log G'$  versus  $\log \omega$  for the 85.5/14.5 Vector 4111/DOP solution during heating at various temperatures: (○) 110 °C; (△) 120 °C; (□) 130 °C; (▽) 135 °C; (◇) 140 °C; (●) 145 °C; (■) 160 °C; (◆) 180 °C; (◐) 190 °C; (▲) 195 °C; (▣) 200 °C; (▼) 205 °C; (◑) 210 °C.

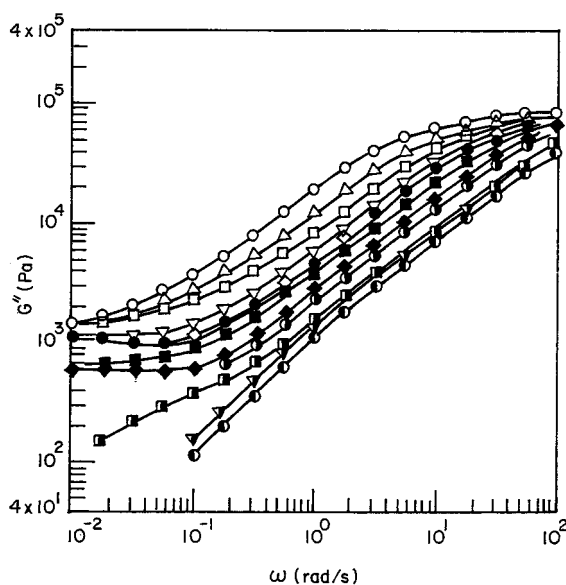


**Figure 12.** Plots of  $\log G''$  versus  $\log \omega$  for the 85.5/14.5 Vector 4111/DOP solution during heating at various temperatures: (○) 110 °C; (△) 120 °C; (□) 130 °C; (▽) 135 °C; (◇) 140 °C; (●) 145 °C; (■) 160 °C; (◆) 180 °C; (◐) 190 °C; (▲) 200 °C; (▼) 205 °C; (◑) 210 °C.

at 150–155 °C. Further, we observe from Figure 10 that  $G'$  begins to decrease rapidly at ca. 200 °C. We are not certain whether this temperature can be regarded as being the  $T_{\text{ODT}}$  of the 85.5/14.5 Vector 4111/DOP solution, because previously<sup>29</sup> we encountered the situation where the temperature at which the value of  $G'$  for neat Vector 4111 began to decrease rapidly did not agree with the  $T_{\text{ODT}}$  determined by other rheological methods.

Figure 11 gives plots of  $\log G'$  versus  $\log \omega$ , and Figure 12 gives plots of  $\log G''$  versus  $\log \omega$ , for the 85.5/14.5 Vector 4111/DOP solution, which were obtained from dynamic frequency sweep experiments during heating from 110 to 210 °C. At present, it is not clear from

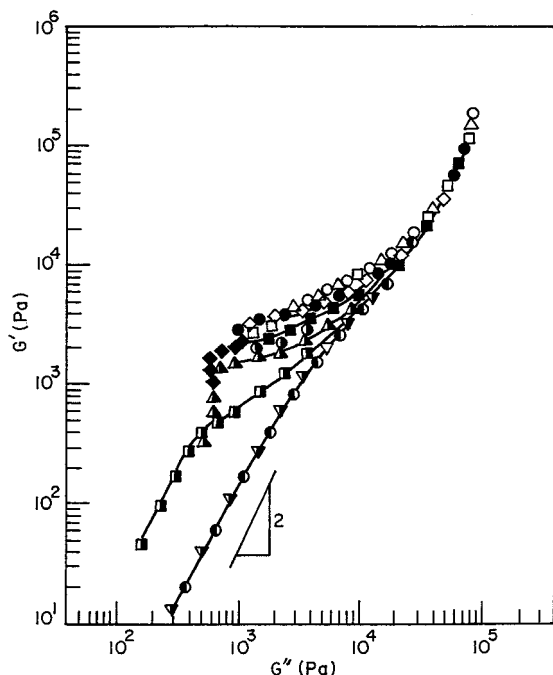


**Figure 13.** Plots of  $\log G'$  versus  $\log G''$  for the 85.5/14.5 Vector 4111/DOP solution during heating at various temperatures: (○) 110 °C; (△) 120 °C; (□) 130 °C; (◇) 140 °C; (●) 145 °C; (■) 160 °C; (◆) 180 °C; (●) 190 °C; (△) 195 °C; (■) 200 °C; (▽) 205 °C; (○) 210 °C.

Figures 11 and 12 show an onset of an OOT and/or an ODT in the 85.5/14.5 Vector 4111/DOP solution can be determined. Thus we prepared plots of  $\log G'$  versus  $\log G''$ , given in Figure 13, using the data in Figures 11 and 12. The following observations are worth noting in Figure 13. (1) Plots of  $\log G'$  versus  $\log G''$  in the terminal region begin to have a slope of 2 at 200 °C and higher temperatures, signifying that the sample exhibits liquid-like rheological behavior. However,  $\log G'$  versus  $\log G''$  plots at 205 and 210 °C overlap, lying on a single correlation, independent of temperature. According to Han and co-workers,<sup>44–46</sup> a threshold temperature at which  $\log G'$  versus  $\log G''$  plots, having a slope 2, in the terminal region become independent of temperature can be regarded as being the  $T_{\text{ODT}}$  of a microphase-separated block copolymer. Thus, we conclude from Figure 13 that the  $T_{\text{ODT}}$  of the 85.5/14.5 Vector 4111/DOP solution is ca. 205 °C. It should be mentioned that there is ample experimental evidence<sup>47</sup> demonstrating that  $\log G'$  versus  $\log G''$  plots in the terminal region of homogeneous, isotropic molten polymers exhibit temperature independence. Theory<sup>48</sup> supports such experimental results.

It should be noted in Figure 13 that  $\log G'$  versus  $\log G''$  plots at 195 °C overlap those at 200 °C for  $G' \approx 300$  Pa. The reason why in Figure 13 there are no more data points which overlap at 195 and 200 °C is not due to the lack of data taken at sufficiently low angular frequencies but due to the rather large value of  $G'$  at 195 °C even for  $\omega = 0.01$  rad/s (see Figure 11), the lowest experimental angular frequency at which one practically runs an oscillatory shear flow experiment.

Earlier, Rosedale and Bates<sup>49</sup> argued that the parallel feature of  $\log G'$  versus  $\log G''$  plots, having a slope of 2, in the terminal region may be attributable to thermal composition fluctuation effects in the disordered (a single phase) state near the  $T_{\text{ODT}}$ . If their argument is applied to Figure 13, we conclude that the thermal fluctuation effects near the  $T_{\text{ODT}}$  of the 85.5/14.5 Vector 4111/DOP solution span ca. 5 °C. This interpretation,

however, is not correct in our system, because at 200 °C we still have spherical microdomains with sharp interface in short range liquid-like spatial order but not thermal composition fluctuations in the disordered state. The rheological behavior is best interpreted as the flow of the spherical microdomains in liquid-like short range spatial order.

Moreover application of Bates' argument to some experimental data in the literature leads us to make inconsistent interpretations. Specifically, nearly symmetric SI diblock or SIS triblock copolymers either show no parallel feature of  $\log G'$  versus  $\log G''$  plots, having a slope of 2, in the terminal region,<sup>46</sup> as reported for the PEP-PEE block copolymers,<sup>49</sup> or show it over a very narrow range of temperatures, say less than 3 °C.<sup>50</sup> On the other hand, highly asymmetric SI diblock or SIS triblock copolymers tend to show the parallel feature of  $\log G'$  versus  $\log G''$  plots, having a slope of 2, in the terminal region over a very wide range of temperature, say as large as 40 °C,<sup>29,50</sup> near  $T_{\text{ODT}}$ . From a physical point of view, one would expect a greater thermal fluctuation effect in symmetric block copolymers in the disordered state than in highly asymmetric block copolymers in the disordered state if two copolymers have the same molecular weight. Therefore, such experimental observations cannot be explained by Bates' argument that the parallel feature of  $\log G'$  versus  $\log G''$  plots, having a slope of 2, in the terminal region may signify the presence of a thermal fluctuation effect near  $T_{\text{ODT}}$  in the disordered state.

Further, in our previous paper<sup>29</sup> we reported that, during heating,  $\log G'$  versus  $\log G''$  plots, having a slope of 2, in the terminal region for Vector 4111, which is a highly asymmetric SIS triblock copolymer, showed no parallel feature at all temperatures ranging from 160 to 220 °C while, during cooling, such plots exhibited the parallel feature, having a slope of 2, at temperatures ranging from 220 to 180 °C. If composition fluctuation effects in the disorder state existed in Vector 4111 and they were manifested by the parallel feature of  $\log G'$  versus  $\log G''$  plots, having a slope of 2, in the terminal region, we should have observed the parallel feature in such plots during both heating and cooling, but we did not.

Therefore, we are of the opinion that the existence of the parallel feature in  $\log G'$  versus  $\log G''$  plots, having a slope of 2, in the terminal region for a highly asymmetric block copolymer has little to do with thermal fluctuation effects near its  $T_{\text{ODT}}$ . As noted in our previous paper,<sup>29</sup> we believe that it is a rheological behavior due to the flow of the spherical microdomains in liquid-like short range spatial order but not due to the concentration fluctuation in the disordered state near the ODT.

**TEM Study.** Figure 14 gives TEM micrographs of 85.5/14.5 Vector 4111/DOP specimens. Each TEM micrograph was taken using a specimen which was annealed at a preset temperature as indicated on the micrograph, with each specimen then being rapidly quenched in ice water. The thermal histories of the specimens employed for taking TEM micrographs are summarized in Table 1. The following observations are worth noting on the TEM micrographs given in Figure 14. (a) The TEM micrograph taken upon quenching from 120 °C, which is ca. 15 °C below the  $T_{\text{OOT}}$  of the specimen, shows hexagonally-packed cylinders of PS. (b) The TEM micrograph taken upon quenching from 145 °C, which is ca. 5 °C above the  $T_{\text{OOT}}$  of the specimen, shows microdomains consisting of spheres of PS in a cubic lattice. (c) The TEM micrograph taken upon



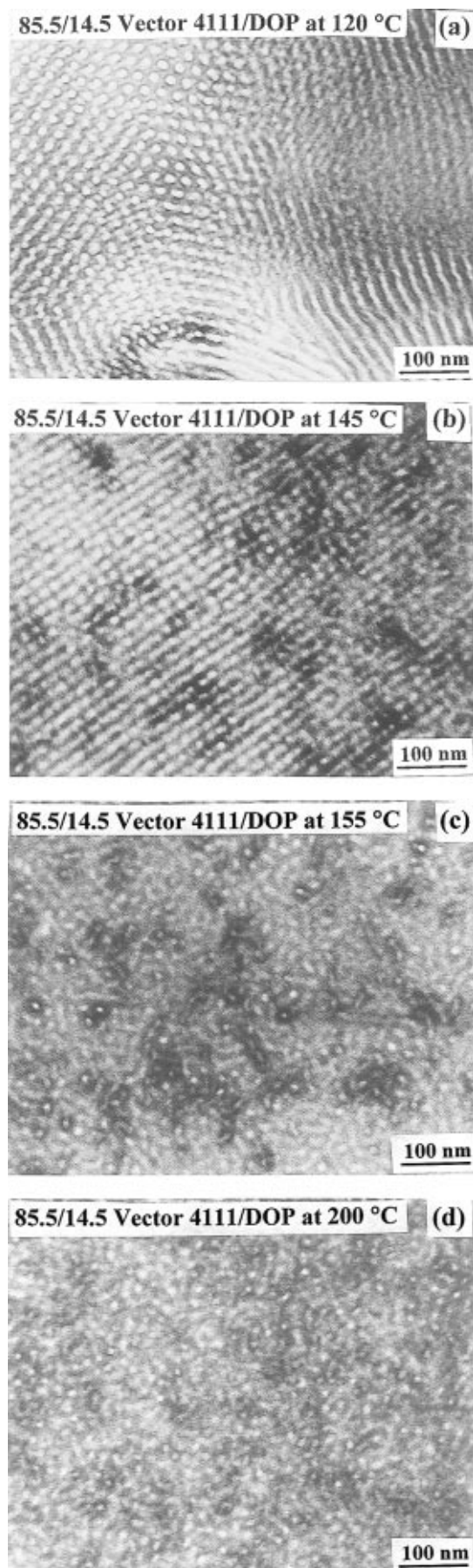


**Figure 14.** Transmission electron micrographs of the 85.5/14.5 Vector 4111/DOP solution at 120, 145, 155, and 200 °C. These micrographs were taken after rapidly quenching the reaction for the specimen from the respective temperatures in ice water, and the thermal histories of the specimens are summarized in Table 1.

quenching from 155 °C, which is just above the  $T_{\text{LDT}}$  of the specimen, shows spherical microdomains with a sharp interface and with a short-range liquid-like order. (d) The TEM micrograph taken upon quenching from 200 °C, which is far above the  $T_{\text{LDT}}$  and just below the assumed  $T_{\text{ODT}}$  of the specimen, shows spherical microdomains still having a sharp interface. These observations completely support the SAXS results presented in Figure 1.

### Concluding Remarks

In this paper, using SAXS, we have observed that the addition of 14.5 wt % DOP lowered the  $T_{\text{OOT}}$  and  $T_{\text{LDT}}$  of Vector 4111 by ca. 50 °C and that the addition of 26.8 wt % DOP lowered the  $T_{\text{OOT}}$  of Vector 4111 by ca. 100 °C. Specifically, we observed from the experiments performed during the heating cycle that (a) hexagonally-packed cylindrical microdomains of PS transform to spherical microdomains of PS at 125–130 °C in the 85.5/14.5 Vector 4111/DOP solution and at 80–90 °C in the 73.2/26.8 Vector 4111/DOP solution and (b) an LDT takes place at 150–155 °C in the 85.5/14.5 Vector 4111/DOP solution, but there is no LDT in the 73.2/26.8 Vector 4111/DOP solution. This suggests that, in the 73.2/26.8 Vector 4111/DOP solution, hexagonally-packed cylindrical microdomains of PS transform directly to the disordered spheres or spheres of PS in a considerably distorted cubic lattice at  $T_{\text{OOT}}$ . The morphologies in the 85.5/14.5 Vector 4111/DOP solution at  $T < T_{\text{OOT}}$ ,  $T_{\text{OOT}} < T < T_{\text{LDT}}$ , and  $T_{\text{LDT}} < T < T_{\text{ODT}}$ , determined by SAXS, were corroborated by TEM. The values of  $T_{\text{OOT}}$  and  $T_{\text{LDT}}$  determined by SAXS measurements for the 85.5/14.5 Vector 4111/DOP solution were corroborated by rheology measurements.

Our previous study<sup>29</sup> indicated that bulk Vector 4111 has a  $T_{\text{ODT}}$  higher than 220 °C, the highest experimental temperature employed without having the possibility of inducing cross-linking reactions. In the present study we have estimated the  $T_{\text{ODT,bulk}}$  of Vector 4111 to be (i) 287 °C from the  $T_{\text{ODT,solution}}$  (205 °C) of the 85.5/14.5 Vector 4111/DOP solution and (ii) 277 °C from the  $T_{\text{ODT,solution}}$  (130 °C) of the 73.2/26.8 Vector 4111/DOP solution, by assuming that DOP strictly plays the role of diluent, i.e., using  $T_{\text{ODT,bulk}} = T_{\text{ODT,solution}}/\phi_p$  with  $\phi_p$  being the volume fraction of the block copolymer in the solution. The estimated values of  $T_{\text{ODT}}$  for bulk Vector 4111 appear to be reasonable.

Finally, we wish to point out that, during heating, an LDT may take place in certain block copolymers before ever reaching the ODT; thus,  $T_{\text{LDT}} < T_{\text{ODT}}$ . In the present study, we observed an LDT taking place in the 85.5/14.5 Vector 4111/DOP solution from SAXS measurements, as in neat Vector 4111.<sup>29</sup> In the 85.5/14.5 Vector 4111/DOP solution we observed spherical microdomains with a sharp interface in short-range liquid-like order, at temperatures between  $T_{\text{LDT}}$  and  $T_{\text{ODT}}$  (i.e.,  $T_{\text{LDT}} < T < T_{\text{ODT}}$ ) from both SAXS and TEM. We emphasize once again that an LDT is an order–disorder transition of spherical microdomains and the LDT and the ODT are identical in the regime where the Landau-type mean-field theory holds. However, for highly *asymmetric* block copolymers (e.g., Vector 4111), spherical microdomains with a long range order (i.e., the lattice) may be destroyed at  $T \geq T_{\text{LDT}}$  but the spheres with a liquid-like short range order persist until reaching  $T_{\text{ODT}}$ , at which point the constituent blocks are mixed on the molecular level and hence no spherical microdomains exist. On the other hand, in the present study we could not discern an LDT taking place in the

73.2/26.8 Vector 4111/DOP solution, which has more DOP in the solution compared to the amount in the 85.5/14.5 Vector 4111/DOP solution. At present it is not clear to us up to what levels of DOP concentration an LDT can be observed in mixtures of Vector 4111 and DOP. In our SAXS measurements, we have *not* observed a sharp and discontinuous change in  $I_m^{-1}$  and  $\sigma_q^2$  near the ODT in both the 85.5/14.5 and 73.2/26.8 Vector 4111/DOP solutions investigated, and thus we inferred the ODT of the solutions from  $D$  versus  $1/T$  plots.

## References and Notes

- Leibler, L. *Macromolecules* **1980**, *13*, 1602.
- Helfand, E.; Wasserman, Z. R. In *Developments in Block Copolymers*; Goodman, I., Ed.; Applied Science: New York, 1982; Chapter 4.
- Arnold, K. R.; Meier, D. J. *J. Appl. Polym. Sci.* **1970**, *14*, 427.
- Ghijssels, A.; Raadsen, *Pure Appl. Chem.* **1980**, *52*, 1359.
- Han, C. D.; Baek, D. M.; Kim, J. K.; Chu, S. G. *Polymer* **1992**, *33*, 294 and references therein.
- Han, J. H.; Feng, D.; Choi-Feng, C.; Han, C. D. *Polymer* **1995**, *36*, 155.
- Zin, W.-C.; Roe, R.-J. *Macromolecules* **1984**, *17*, 183. (b) Nojima, S.; Roe, R.-J. *Macromolecules* **1987**, *20*, 1866.
- (a) Kim, J.; Han, C. D.; Chu, S. G. *J. Polym. Sci., Polym. Phys. Ed.* **1988**, *26*, 677. (b) Han, C. D.; Kim, J.; Baek, D. M.; Chu, S. G. *J. Polym. Sci., Polym. Phys. Ed.* **1990**, *28*, 315.
- Hashimoto, T.; Tanaka, H.; Hasegawa, H. *Macromolecules* **1990**, *23*, 4378.
- Tanaka, H.; Hasegawa, H.; Hashimoto, T. *Macromolecules* **1991**, *24*, 240.
- Tanaka, H.; Hashimoto, T. *Macromolecules* **1991**, *24*, 5713.
- Winey, K. I.; Thomas, E. L.; Fetters, L. J. *J. Chem. Phys.* **1991**, *95*, 9367.
- Hashimoto, T.; Koizumi, S.; Hasegawa, H.; Izumitani, T.; Hyde, S. T. *Macromolecules* **1992**, *25*, 1433. Koizumi, S.; Hasegawa, H.; Hashimoto, T. *Makromol. Chem., Macromol. Symp.* **1992**, *62*, 75. Koizumi, S.; Hasegawa, H.; Hashimoto, T. *Macromolecules* **1994**, *27*, 6532.
- Baek, D. M.; Han, C. D.; Kim, J. K. *Polymer* **1992**, *33*, 4821.
- Han, C. D.; Baek, D. M.; Kim, J.; Kimishima, K.; Hashimoto, T. *Macromolecules* **1992**, *25*, 3052.
- Winey, K. I.; Thomas, E. L.; Fetters, L. J. *Macromolecules* **1992**, *25*, 422.
- Disko, M. M.; Liang, K. S.; Behal, S. K.; Roe, R. J.; Jeon, K. J. *Macromolecules* **1993**, *26*, 2983.
- Spontak, R. J.; Smith, S. D.; Ashraf, A. *Macromolecules* **1993**, *26*, 5118.
- Kraus, G.; Hal, D. S. In *Block Copolymers—Science and Technology*; Meier, D. J., Ed.; MMI Symposium Series vol. 3; Harwood Academic: New York, 1983; p 129.
- Kraus, G.; Hashimoto, T. *J. Appl. Polym. Sci.* **1982**, *27*, 1745.
- Sakurai, S.; Hashimoto, T.; Fetters, L. J. *Macromolecules* **1996**, *29*, 740.
- Almdal, K.; Koppi, K. A.; Bates, F. S.; Mortensen, K. *Macromolecules* **1992**, *25*, 1743.
- Sakurai, S.; Momii, T.; Taie, K.; Shibayama, M.; Nomura, S.; Hashimoto, T. **1993**, *25*, 458.
- Sakurai, S.; Kawada, H.; Hashimoto, T.; Fetters, L. *Macromolecules* **1993**, *26*, 5796.
- Hamley, I. W.; Koppi, K. A.; Rosedale, J. H.; Bates, F. S.; Almdal, K.; Mortensen, K. *Macromolecules* **1993**, *26*, 5659.
- Förster, S.; Khandpur, A. K.; Zhao, J.; Bates, F. S.; Hamley, I. W.; Ryan, A. J.; Bras, W. *Macromolecules* **1994**, *27*, 6922.
- Hajduk, D. A.; Gruner, S. M.; Rangarajan, P.; Register, R. S.; Fetters, L. J.; Honeker, C.; Albalak, R. J.; Thomas, E. L. *Macromolecules* **1994**, *27*, 490.
- Khandpur, A. K.; Förster, S.; Bates, F. S.; Hamley, I. W.; Ryan, A. J.; Bras, W.; Almdal, K.; Mortensen, K. *Macromolecules* **1995**, *28*, 8796.
- Sakamoto, N.; Hashimoto, T.; Han, C. D.; Kim, D.; Vaidya, N. Y. *Macromolecules* **1997**, *30*, 1621.
- Hashimoto, T.; Shibayama, M.; Kawai, H.; Watanabe, H.; Kotaka, T. *Macromolecules* **1983**, *16*, 361.
- Schwab, M.; Stühn, B. *Phys. Rev. Lett.* **1996**, *76*, 924.
- Fredrickson, G. H.; Helfand, E. *J. Chem. Phys.* **1987**, *87*, 697.
- Hashimoto, T.; Shibayama, M.; Kawai, H. *Macromolecules* **1983**, *16*, 1093. We usually determined the neutrality of the solvent against the two block chains under consideration by measuring the concentration dependence of the volume ratio of two lamellar microphases. If there is no concentration dependence in the volume ratio, the solvent was judged as neutral (see for example the work by Sakurai et al.<sup>34</sup>).
- Sakurai, S.; Mori, K.; Okawara, A.; Kimishima, K.; Hashimoto, T. *Macromolecules* **1992**, *25*, 2679.
- (a) Hashimoto, T.; Suehiro, S.; Shibayama, M.; Saijo, K.; Kawai, H. *Polym. J.* **1981**, *13*, 501. (b) Suehiro, S.; Saijo, K.; Ohta, Y.; Hashimoto, T.; Kawai, H. *Anal. Chim. Acta* **1986**, *189*, 41.
- Fujimura, M.; Hashimoto, T.; Kawai, H. *Mem. Fac. Eng., Kyoto Univ.* **1981**, *43* (2), 224.
- Hendricks, R. W. *J. Appl. Crystallogr.* **1972**, *5*, 315.
- Hashimoto, T.; Fujimura, M.; Kawai, H. *Macromolecules* **1980**, *13*, 1660.
- Sakamoto, N.; Hashimoto, T. *Macromolecules* **1995**, *28*, 6825.
- Helfand, E.; Tagami, Y. *J. Chem. Phys.* **1972**, *56*, 3573.
- Onuki, A.; Hashimoto, T. *Macromolecules* **1989**, *22*, 879.
- Hashimoto, T.; Mori, K. *Macromolecules* **1990**, *23*, 5347.
- Lodge, T. P.; Pan, C.; Jin, X.; Liu, Z.; Zhao, J.; Maurer, W. W.; Bates, F. S. *J. Polym. Sci., Polym. Phys. Ed.* **1995**, *33*, 2289.
- Hosemann, R.; Bagchi, S. N. In *Direct Analysis of Diffraction by Matter*; North-Holland Publishing Company: Amsterdam, 1962; Chapter IX.
- Han, C. D.; Kim, J. *J. Polym. Sci., Polym. Phys. Ed.* **1987**, *25*, 1741.
- Han, C. D.; Kim, J.; Kim, J. K. *Macromolecules* **1989**, *22*, 383.
- Han, C. D.; Baek, D. M.; Kim, J. K. *Macromolecules* **1990**, *23*, 561.
- Han, C. D.; Lem, K.-W. *Polym. Eng. Rev.* **1982**, *2*, 135. (b) Chuang, H.-K.; Han, C. D. *J. Appl. Polym. Sci.* **1984**, *29*, 2205. (c) Han, C. D.; Yang, H. H. *J. Appl. Polym. Sci.* **1987**, *33*, 1221. (d) Han, C. D. *J. Appl. Sci.* **1988**, *35*, 167.
- Han, C. D.; Jhon, M. S. *J. Appl. Polym. Sci.* **1986**, *32*, 3809. (b) Han, C. D.; Kim, J. K. *Macromolecules* **1989**, *22*, 4292.
- Rosedale, J. H.; Bates, F. S. *Macromolecules* **1990**, *23*, 2329.
- Han, C. D.; Baek, D. M.; Kim, J. K.; Ogawa, T.; Sakamoto, N.; Hashimoto, T. *Macromolecules* **1995**, *28*, 5043.

MA961696C